Journal of Biomolecular NMR **30:** 163–173, 2004.

NMR structure of a complex between MDM2 and a small molecule inhibitor

David C. Fry[a,*], S. Donald Emerson[a,c], Stefan Palme[b], Binh T. Vu[a], Chao-Min Liu[a] & Frank Podlaski[a]

[a]*Roche Research Center, Hoffmann-La Roche, Inc. 340 Kingsland Street, Nutley, NJ 07110, U.S.A.;* [b]*Pharma Research, Roche Diagnostics GmbH, Nonnenwald 2, D-82377 Penzberg, Germany;* [c]*Current address: Discovery Technologies, Pfizer, Inc., 2800 Plymouth Road, Ann Arbor, MI 48105, U.S.A.*

Received 11 March 2004; Accepted 31 May 2004

Key words: MDM2, NMR spectroscopy, protein-protein interaction, protein structure

Abstract

MDM2 is a regulator of cell growth processes that acts by binding to the tumor suppressor protein p53 and ultimately restraining its activity. While inactivation of p53 by mutation is commonly observed in human cancers, a substantial percentage of tumors express wild type p53. In many of these cases, MDM2 is overexpressed, and it is believed that suppression of MDM2 activity could yield therapeutic benefits. Therefore, we have been focusing on the p53-MDM2 interaction as the basis of a drug discovery program and have been able to develop a series of small molecule inhibitors. We herein report a high resolution NMR structure of a complex between the p53-binding domain of MDM2 and one of these inhibitors. The form of MDM2 utilized was an engineered hybrid between the human and Xenopus sequences, which provided a favorable combination of relevancy and stability. The inhibitor is found to bind in the same site as does a highly potent peptide fragment of p53. The inhibitor is able to successfully mimic the peptide by duplicating interactions in three subpockets normally made by amino acid sidechains, and by utilizing a scaffold that presents substituents with rigidity and spatial orientation comparable to that provided by the alpha helical backbone of the peptide. The structure also suggests opportunities for modifying the inhibitor to increase its potency.

Introduction

The oncogene first identified as mouse double minute 2 ('MDM2') has emerged as a potential target for anti-cancer therapy (Zheleva et al., 2003). MDM2 represses p53 activity in multiple ways. It serves as an E3 ubiquitin ligase which binds directly to p53 and targets it for destruction (Haupt et al., 1997; Kubbutat et al., 1997; Midgley and Lane, 1997). MDM2 also inhibits via direct blockage of the domain of p53 which mediates its function as a transcription activator (Oliner et al., 1992). With reduced p53 activity, defective cells, for example those with damaged DNA, will more likely proliferate than undergo apoptosis (Levine, 1997). The p53 protein is recognized as one of the dominant tumor suppressors, and its mutation to an inactive form is one of the most common genetic alterations observed in human cancers (Hollstein et al., 1991). However, a substantial percentage of cancer cells express wild type p53, although it is believed that the p53 activity may still be in a depressed state via some secondary mechanism (Oliner et al., 1992). In certain tumors containing wild type p53, it has been found that MDM2 is overexpressed (Oliner et al., 1992). These tumors cover a range of tissue types, including connective tissue, brain, esophagus, and breast (Reifenberger et al., 1993; Bueso-Ramos et al., 1993; Shibagaki et al., 1995; Marchetti et al., 1995). It is believed that for this class of tumors, suppression of MDM2 activity could enhance the growth-suppressing

*To whom correspondence should be addressed. E-mail: david.fry@roche.com

effects of p53, ultimately resulting in a therapeutic benefit. Toward this end, we have been focusing on the p53-MDM2 interaction as the basis of a drug discovery program.

The p53-MDM2 interaction has been well characterized at a molecular level. The domain of MDM2 that binds to p53 is contained within its first 120 N-terminal residues (Chen et al., 1993). The region of p53 that participates in the interaction is even smaller – a peptide fragment comprised of residues 15–29 is able to efficiently compete with the intact protein for binding (Picksley et al., 1994). X-ray structures have been reported for p53 peptides in complex with the binding domain of MDM2 from two species, human (residues 17-125) and Xenopus (residues 13–119) (Kussie et al., 1996). These structures revealed that the p53 peptide adopts a helical structure when bound and inserts three hydrophobic side chains into sub-pockets of the MDM2 site. In this structure, the dimensions of the binding interface appeared relatively compact, suggesting that a small organic molecule might be able to mimic enough of the critical interactions to act as a high affinity inhibitor of the interaction.

Small molecule inhibitors of protein-protein interactions have been described, but are relatively rare (Toogood, 2002; Berg, 2003). While pioneering studies on the human growth hormone system showed that in certain cases such inhibitors should, in principle, be obtainable (Clackson and Wells, 1995), most protein-protein interactions involve large binding sites where affinity is obtained by a multitude of weak interactions. These widely-spaced interactions cannot be duplicated by a small molecule. Even more rare have been cases where a reported small molecule inhibitor has been drug-like. While a number of reports have described elegant work resulting in the discovery of reasonably small organic molecules as protein-protein inhibitors (Berg et al., 2002; Carter et al., 2001; McMillan et al., 2000; Orner et al., 2001; Smith et al., 1997; Lunney et al., 1997; Proudfoot et al., 1002; Bohacek et al., 2001; Zhu et al., 2003), these molecules were not meant to be drug-like and in this regard possess liabilities – such as charged groups, an excessive number of rotatable bonds, or too much peptidic character. Examples of systems for which drug-like inhibitors have been demonstrated are: the interaction of the cell adhesion proteins GPIIbIIIa, LFA-1, and VLA-4 with their respective partners fibrinogen, ICAM-1, and VCAM-1 (McDowell et al., 1994; Ku et al., 1993; Kallen et al., 1999; Gadek et al., 2002; Liu et al., 2001; Last-Barney et al., 2001; Chen et al., 2002), the interaction of the apoptotic protein Bcl-XL with its regulatory partner Bak (reviewed in: Rutledge et al., 2002), the association of the cytokine Interleukin-2 with its receptor (Tilley et al., 1997; Braisted et al., 2003), and the interaction of the mediator complex protein Sur-2 with its activator ESX (Asada et al, 2003). There have also been reports of drug-like small molecule inhibitors of the MDM2-p53 interaction, although these were exceedingly weak binders (Stoll et al., 2001). For most of these protein-protein systems, structures are available only for the apo version of the protein targeted by the inhibitor or for a version complexed with a natural ligand. In the case of LFA-1, extensive NMR and X-ray structural studies have characterized complexes with inhibitors bound (Kallen et al., 1999; Liu et al., 2001; Last-Barney et al., 2001), but these drug-like inhibitors were found to bind at a site different from that utilized by the natural ligand. For Interleukin-2, complexes of the target protein with inhibitors bound have been structurally characterized by NMR mapping and X-ray crystallography (Emerson et al., 2003; Arkin et al., 2003), but a detailed structure of the target with its receptor has not been obtained. None of these cases provides the combination of structures allowing one to directly compare complexes between the target and its artificial and natural ligands. Such a comparison could address the prevalent suspicion that inhibitors of protein-protein interactions are rare because there is some special quality of a proteinaceous ligand that cannot be duplicated by a non-protein molecule.

In this report, we present a high-resolution NMR structure of a complex between MDM2 and a drug-like small molecule inhibitor. Since an X-ray structure of MDM2 is available as a complex with a peptide fragment of p53, its natural ligand, we are able to examine in detail how a small drug-like inhibitor is able to mimic a peptide substrate. The analysis shows that although the peptide is much larger, parts of it are not directly essential and the functions of these parts can be duplicated in a more economical manner by the small inhibitor. The structure is also employed to suggest strategies for modifying the inhibitor to increase its potency.

Materials and methods

Expression and purification

The plasmid containing the sequence of Xenopus MDM2 (13-119) was obtained using standard methods (to be published elsewhere). The gene sequence coding for the desired protein fragment was amplified by PCR and cloned into an expression vector derived from plasmid pQ40 (Qiagen). The mutations I50L, P92H, L95I to create a 'humanized' xenopus MDM2 (13-119) were introduced by site directed mutagenesis using overlap extension PCR (Higuchi et al., 1988; Ho et al., 1989). Appropriate mutagenesis primers were purchased from MWG Biotech, Germany.

Proteins were expressed in E. coli strain BL21 using the helper plasmid pUBS 520 coding for the $lacI^q$ repressor and the rare $tRNA^{Arg}$ [AGA/AGG] (Brinkmann et al., 1989). Cells were grown at 37 °C in minimal fermentation medium containing 2 g/l ^{15}N-NH_4Cl for ^{15}N-single labeled, or 2 g/l ^{15}N-NH_4Cl and 2 g/l ^{13}C-Glucose for $^{15}N/^{13}C$-double labeled, protein. Expression was induced by 1 mM IPTG. Cells were centrifuged and resuspended in 0.1 M Tris/HCl pH 7.0, with addition of lysozyme and DNAse. After cell disruption by high pressure dispersion ('French press'), inclusion bodies were separated by centrifugation, washed with a) 30 g/l Brij 35, 0.75 M NaCl, 30 mM EDTA, pH 7.0 and b) 0.1 M Tris/HCl, 20 mM EDTA, pH 6.5 and solubilized in 6 M GdnHCl, 100 mM Tris/HCl, 5 mM EDTA, 10 mM DTT, pH 7.5. Refolding was accomplished by slowly diluting the solubilized protein 100-fold into 50 mM MES, 50 mM NaCl, 1 mM EDTA and 5 mM DTT, pH 7.0 at room temperature. After removal of insoluble material, ammonium sulfate was added to a final concentration of 1.5 M. Protein was adsorbed on Butyl-Sepharose 4 fast flow (Amersham Biosciences), washed with high-salt buffer (25 mM MES, 1.5 M Ammonium sulfate, 1 mM EDTA, pH 7.0) and eluted with 25 mM MES, 1 mM EDTA, pH 7.0. After adjusting the pH to 6.5 (HCl), further purification was performed by cation exchange chromatography on SP-Sepharose (Amersham Biosciences) at 4 °C applying a gradient from 0–500 mM NaCl. Finally, the protein was gel-filtrated on a high load Superdex 75 column (Amersham Biosciences) using 100 mM potassium phosphate, 1 mM EDTA, and 2 mM DTT, pH 7.0.

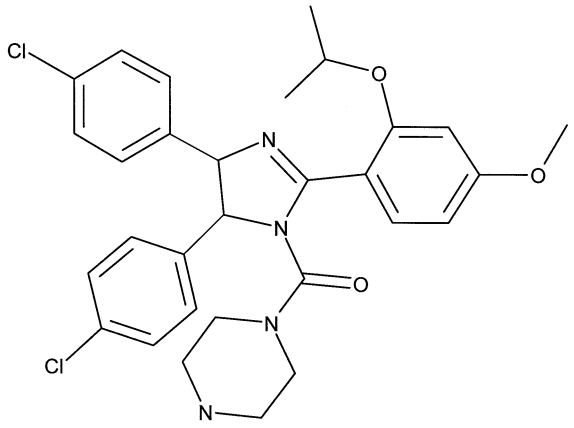

Compound 1

Figure 1. The primary structure of Compound **1** – an inhibitor of the MDM2-p53 interaction.

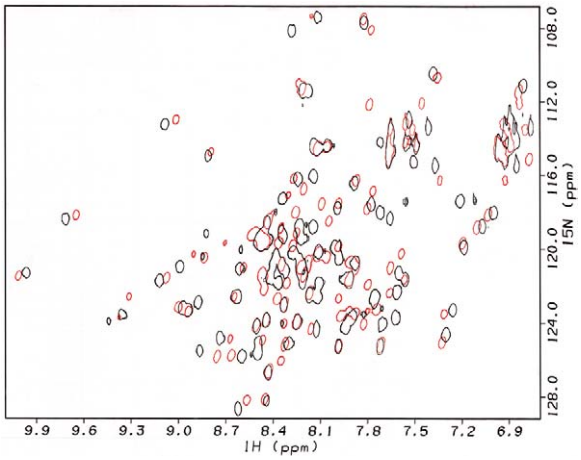

Figure 2. Superposition of 2D ^1H-^{15}N-HSQC spectra of ^{15}N-labeled hx-MDM2 alone (black) and in complex with Compound **1** (red).

*Synthesis and affinity of compound **1***

Compound **1** (Figure 1) was prepared as illustrated in Scheme 1. 3-Methoxyphenol was first brominated then the corresponding bromide **2** was alkylated to give 1-bromo-2-isopropoxy-4-methoxybenzene (**3**). Palladium catalyzed cyanation of **3** and treatment of the cyanide with hydrogen chloride in ethanol provided the imidate **4**. The imidate **4** was coupled with *meso*-(4-chlorophenyl)ethane-1,2-diamine (**5**) (Vogtle and Goldschmitt, 1976; Jennerwein et al., 1988) to give the imidazoline intermediate **6**. Treatment of **6** with phosgene and reaction of the

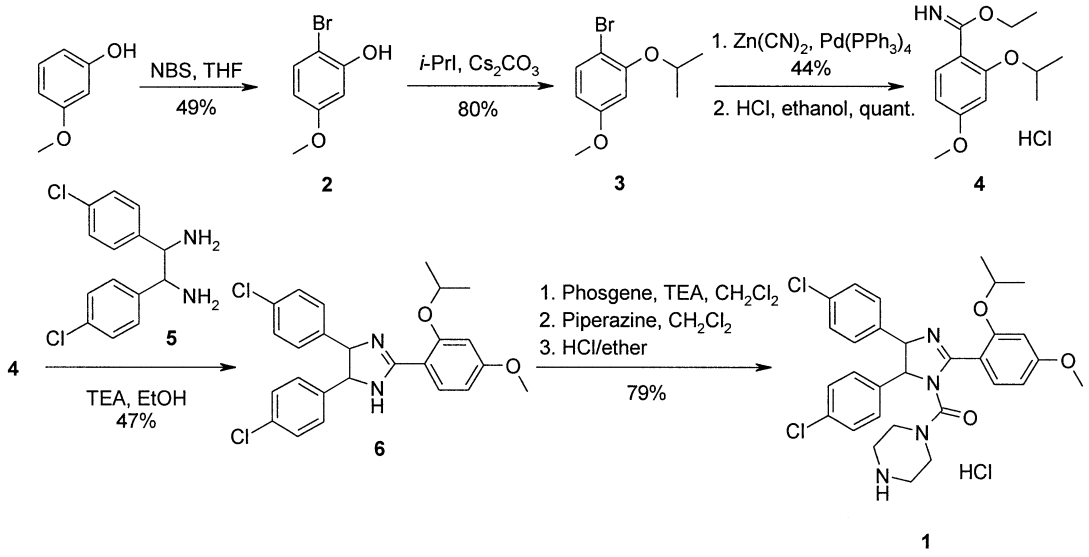

Scheme 1.

resulting carbamoyl chloride with piperazine afforded **1** as hydrochloride salt.

The inhibitory activity of Compound **1** against human MDM2 was measured in a competition assay using the p53 peptide, and its IC_{50} value was found to be 160 nM.

NMR spectroscopy

The NMR samples contained 0.6 mM ^{15}N- or ^{13}C/^{15}N-labeled hx-MDM2, with Compound **1** added to a concentration of 3.5 mM in order to ensure saturation. The buffer system was 50 mM MES-d13 (Cambridge Isotope Labs) pH 7.0; 150 mM KCl; 50 mM DTT-d10 (Cambridge Isotope Labs); 1.5 mM NaN_3. The volume of sample was 630 µl in a 5 mm Wilmad 535-PP NMR tube.

NMR experiments were run on a Varian Inova 600 at 20 °C, using a triple-resonance probe, and pulsed-field Z-axis gradients. Chemical shift assignments and acquisition of NOEs were accomplished using a series of heteronuclear 2D and 3D experiments, according to standard strategies (Clore and Gronenborn, 1994). The 2D ^{1}H-^{15}N HSQC, 3D ^{1}H-^{1}H-^{15}N NOESY-HSQC, and 3D ^{1}H-^{1}H-^{15}N TOCSY-HSQC experiments utilized a sensitivity-enhanced phase-sensitive pulsed field gradient approach for water suppression and selection of the heteronuclear coherence pathway (Kay et al., 1992; Stonehouse et al., 1994). The P and N data were collected as separate hypercomplex pairs and combined to produce the phase sensitive spectrum (Nagayama, 1986). The 3D spectra were acquired with soft preirradiation ($\gamma H_2 = 20$ Hz) for 1.2 s in order to suppress exchange peaks from H_2O to H^N which obscure crosspeaks to H^αs that resonate at the water frequency. In addition, while shifted pulses were used to excite the NH region, the carrier frequency was placed on the water resonance, allowing zero-frequency subtraction during processing, followed by appropriate shifting of the spectrum to provide a normal view of the NH region. The TOCSY experiment was acquired by co-adding four MLEV-17 spin-lock times: 25 ms, 38 ms, 54 ms, and 70 ms The NOESY experiment utilized a mixing time of 125 ms. The 3D ^{1}H-^{1}H-^{13}C HCCH-TOCSY (Bax et al., 1990) spectrum was acquired using co-added DIPSI-3 (Shaka et al., 1988) spin locks of 15.2 ms and 22.8 ms. The 3D HNCACB and CBCACONH experiments (Muhandiram and Kay, 1994) were acquired with the ^{13}C transmitter placed in the center of the ^{13}CO region to facilitate selective decoupling of ^{13}CO carbons with the SEDUCE-1 scheme (McCoy and Mueller, 1992), while the $^{13}C^{\alpha}$ pulses were given as shifted pulses at 46 ppm. The ^{1}H-^{1}H-^{13}C-NOESY-HMQC experiment was collected in two forms, optimizing aliphatic and aromatic protons respectively. The mixing times were 125 ms. Intermolecular NOEs between MDM2 and Compound **1** were obtained with a ^{13}C/^{15}N-filtered 2D NOESY experiment run in hypercomplex phase-sensitive mode (Ikura and Bax, 1992) using the double-labeled protein and unlabeled ligand. This experiment was run in two ways, with ^{13}C and ^{15}N decoupled respectively,

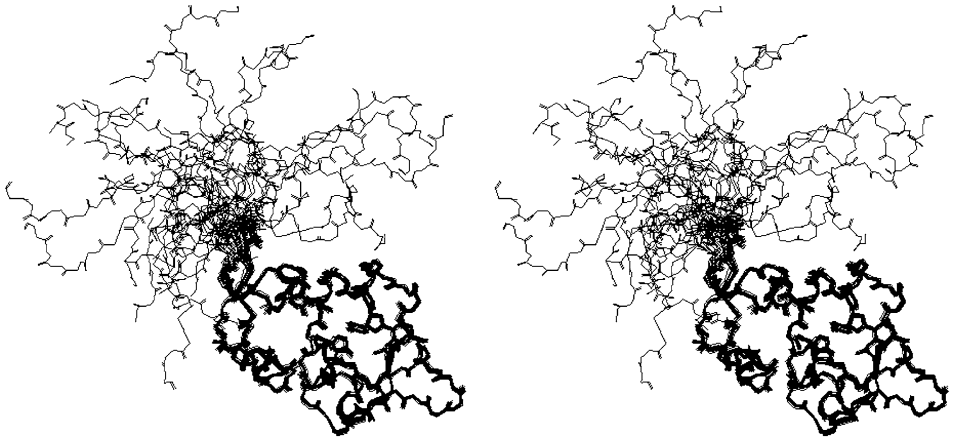

Figure 3. Stereoview showing a superposition of the ensemble of eighteen structures of hx-MDM2 complexed with Compound **1** as determined by NMR. For the protein, only the backbone atoms are depicted. The structures were aligned to optimize the superposition of the structured region (residues 21–105).

in order to differentiate NOEs to carbon- vs. nitrogen-bound protons. Assignments of Compound **1** were assisted by comparison to 2D COSY and TOCSY experiments run on a sample of the free compound in the same buffer system.

Data were processed using FELIX (Accelrys) and analyzed using NMRView (Johnson and Blevins, 1994).

Structure calculations

NOE volumes were measured using NMRView and converted into distance constraints using the standard $1/r^6$ relationship, standardized by a collective consideration of NOEs involving protons whose distance apart is fixed within a narrow range (Emerson et al., 1995). In order to apply the distance constraints in a conservative manner, to allow for uncertainties in NOE measurements and the assumptions inherent in the distance calibrations, we added relatively large uncertainty ranges of +/− 30%. Intermolecular NOEs were identified and assigned in the 2D XY-filtered experiments. For those that were also clearly visible in the 3D NOESY experiments, distances were derived from volumes in the 3D experiments. Further, an appropriate conversion factor was derived from these NOEs, in order to convert volumes to distances for the NOEs observed more clearly in the 2D XY-filtered experiments.

Structures were calculated with the program CNX (Accelrys – Version 2002), using standard protocols (Nilges et al., 1988a, 1988b). Appropriate parameters for Compound **1** were added to the standard protein parameter file. An initial input structure of the MDM2-Compound **1** complex was created by building Compound **1** in the program Insight (Accelrys), and then docking it into the X-ray structure of hx-MDM2 (to be published elsewhere) while loosely applying several key intermolecular distance constraints, using the program MOE (Chemical Computing Group). The X-ray structure of hx-MDM2 that was utilized was originally solved with a peptide bound to the active site, which was removed to allow docking of Compound **1**. Dihedral angle constraints were obtained from analysis of N, Cα, Cβ, and Hα chemical shifts using the program TALOS (Cornilescu et al., 1999). Dihedral angle constraints were applied if they were classified as 'Good' predictions by TALOS, unless preliminary structures produced a dihedral angle that was substantially different from the predicted one. Uncertainty ranges for dihedral angle constraints were set at +/− 30°. After preliminary structures were determined, hydrogen bonds that were consistently observed were added as constraints. Hydrogen bond constraints were incorporated in the standard manner, by applying two distances: HN − O = 1.8 −0.3/+0.7 Å and N − O = 2.8 −0.4/+0.7 Å. A list of all constraints, with the total number of each type, is presented in Table 1. Forty-two structures were calculated, and the eighteen with the best agreement to the experimental NOE constraints were kept. The quality of the structures was assessed using the programs ProcheckNMR (Laskowski et al., 1996) and Xplor (Accelrys).

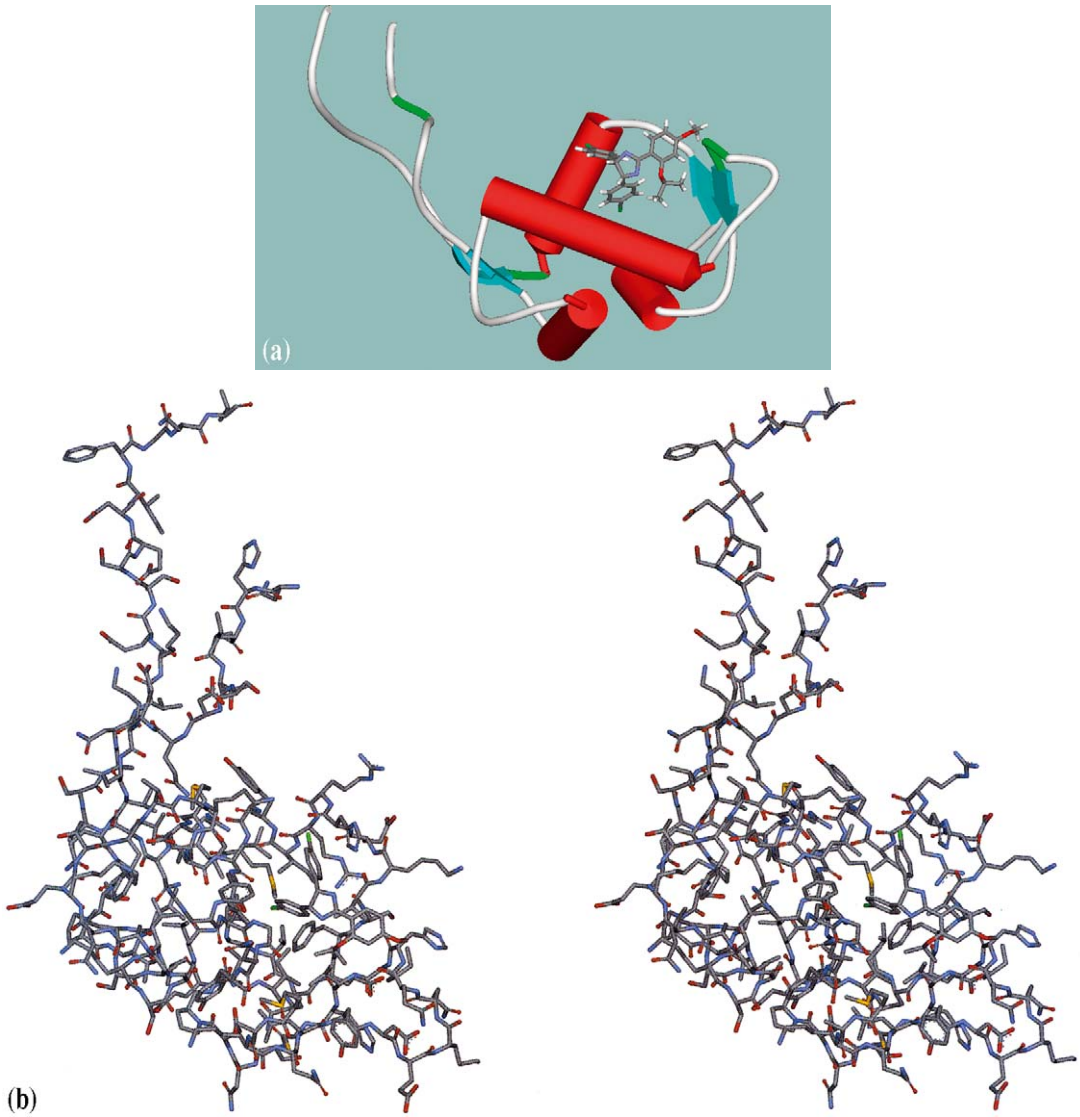

Figure 4. (a) A representative structure from the ensemble, in which the protein backbone is depicted in schematic form, and Compound **1** is depicted in stick form. (b) Stereoview of the structure, with side-chains, colored by atom type.

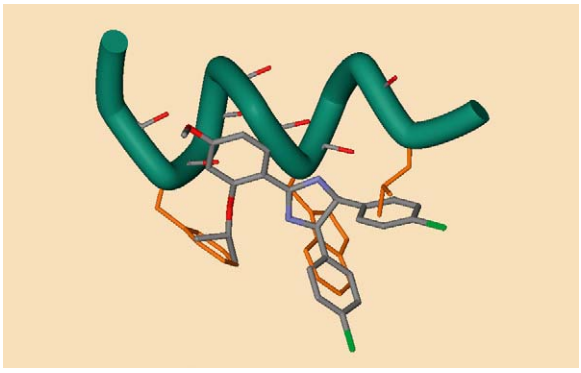

Figure 5. Superposition of Compound **1** bound to hx-MDM2 as determined in the present study by NMR, and the p53 peptide bound to Xenopus-MDM2 as determined previously by X-ray crystallography (Kussie et al., 1996). The figure was prepared by aligning the two protein complex structures, so as to optimize the superposition of residues at the active site: L50, L53, I57, M58, Y63, V71, F82, F87, V89, I95, and M98 (hx-MDM2 numbering). Atoms were then hidden, with the exception of: Compound **1** (colored by atom type, depicted in stick form); the three side chains of the p53 peptide known to be critical for activity (colored orange; from left to right: Phe19, Trp23, Leu26); and the backbone carbonyl atoms of the p53 peptide (colored red). The backbone of the p53 peptide is depicted in tube form and colored green. This overlay shows how the small molecule inhibitor is able to mimic the key side chains of the natural peptide ligand, without directly duplicating the backbone.

Table 1. NMR-derived constraints and structural statistics[a]

Number of experimental constraints		
NOE-based distance constraints:		
Intraresidue ($\Delta = 0$)	482	
Sequential ($\Delta = 1$)	267	
Medium range ($\Delta = 2$ to 4)	204	
Long range ($\Delta > 4$)	157	
Inhibitor: intramolecular	5	
Inhibitor: intermolecular	54	
Total	1169	
Dihedral angle constraints:	176	
Hydrogen bond constraints:	48	
Structural statistics		
RMSD from experimental data		
NOES (Å)	0.0123	± 0.0005
Dihedrals (deg)	0.414	± 0.003
H-Bonds (Å)	0.0049	± 0.0015
RMSD from the mean structure (Å)[b]		
Backbone	0.358	± 0.058
All heavy atoms	0.863	± 0.054
RMSD from ideal geometry		
Bonds (Å)	0.0016	± 0.0001
Angles (deg)	0.337	± 0.005
Impropers (deg)	0.192	± 0.009
Energies (kcal/mol)		
Overall	120.3	± 4.3
Bond	4.66	± 0.26
Angle	55.9	± 1.6
Improper	5.22	± 0.49
van der Waals	36.4	± 2.1
NOE	14.3	± 0.8
Dihedral	3.70	± 0.46
Lennard-Jones[c]	−408.0	± 20.7
Ramachandran plot analysis:		
Most Favored	82.3%	
Allowed	15.5%	
Generously allowed	1.3%	
Disallowed	1.0%	

[a]For the ensemble of 18 structures.
[b]Calculated for the structured region (residues 21–105).
[c]The Lennard–Jones potential van der Waals energy was calculated using the CHARMm parameters in the program Insight2000. It was not employed during the structure calculations.

Results and discussion

Use of a humanized-xenopus MDM2 hybrid

Preliminary NMR studies with the human protein (residues 1–118) indicated that it was not very stable in terms of behavior in an NMR tube, and precipitated over time. The Xenopus form of MDM2 (residues 13–119) was found to be much more stable. The binding affinity of the Xenopus protein, with respect to the human p53 peptide and derivatives thereof, was found to be only about six-fold weaker than that of the human protein. However, for the purposes of drug discovery, our target is the human form of MDM2. As a compromise, a hybrid version of the protein was created, designated 'humanized-Xenopus-MDM2' ('hx-MDM2'), which consisted of residues 13–119 of the Xenopus sequence with three amino acid changes in the active site, corresponding to residues found in those positions in the human sequence. These changes were: Ile50 to Leu; Pro92 to His; and Leu95 to Ile. The stability characteristics of hx-MDM2 were found to be intermediate between those of the human and Xenopus forms. Stability was assessed by measuring the signal volumes over time in 2D ^{1}H-^{15}N-HSQC experiments for an individual NMR sample of each of the three forms, with no ligands added, maintained at 22 °C. The half-time for signal disappearance was found to be 130 days for Xenopus, 5 days for human, and 24 days for humanized-Xenopus. The binding attributes of hx-MDM2, in terms of affinity for the p53 peptide and derivatives thereof, were also found to be about midway between those of the human and Xenopus forms. This was viewed as an acceptable compromise in order to obtain high-quality NMR data, with the belief that, in the early stages of drug design, structure-guided alterations to Compound **1** meant to evoke gross improvements in affinity would most likely be realized for both the Xenopus and human binding sites.

Chemical shift assignments and structure determination

The hx-MDM2 sample produced NMR spectra that were well resolved, and the spectral quality remained high upon complexation with Compound **1**. Chemical shift perturbations of labeled hx-MDM2 were used to verify binding of Compound **1** (as exemplified for the NH groups in Figure 2) and to assess what concentration ratio would insure saturation. The extent of perturbation indicated binding at a single discrete site, with possible small adjustments at more

remote regions but without induction of any major conformational changes in the protein fold. In accord with their lack of significance, chemical shift changes for residues beyond the active site were similar to those observed upon complexation with the p53 peptide. Chemical shift assignments were accomplished by acquiring a set of 3D triple resonance experiments, and determining intraresidue and interresidue through-bond connectivities according to well established strategies (Clore and Gronenborn, 1994). Complete assignments were obtained for all backbone and side-chain ^{1}H, protonated ^{13}C, and protonated ^{15}N atoms, with the exception of all atoms of the N-terminal residue Asn13, and the CαH protons of Asn75 and Gln85. The ^{1}H atoms of bound Compound **1** were also assigned, using the XY-filtered NOESY, assisted by comparison to assignments made for a separate sample of free Compound **1** in the same buffer using standard 2D^{1}H-^{1}H COSY and TOCSY analysis.

Structures were calculated using the program CNX, employing standard protocols (Nilges et al., 1988a, 1988b). Preliminary structures were determined by applying only NOE-derived distance constraints. Inspection of these structures indicated where it was appropriate to add dihedral angle constraints, based on predictions using chemical shifts, and hydrogen bond constraints. In a subsequent stage, forty two structures were calculated, sufficient to establish that agreement to the experimental NOEs was being achieved, as judged by the ENOE energies from CNX clustering into an acceptable range, without extreme excursions beyond this range. The eighteen structures with the best agreement to the experimentally-determined constraints were kept. Statistics indicating the quality and similarity of these structures are shown in Table I. The structures exhibit acceptable geometry with respect to idealized values, and the majority of the backbone dihedral angles are in the favored and acceptable ranges. The structured regions of the protein (residues 21–105) are well-determined, with a low degree of variation among the ensemble of calculated structures (Figure 3). The N- and C-termini are less well-determined, vary widely among the ensemble, and therefore appear to be flexible.

*General structural features of the complex between hx-MDM2 and compound **1***

The overall structure of the protein moiety in the structure reported here (Figure 4) is quite similar to the one reported for the p53-peptide complexes (Kussie et al., 1996), consisting of a base formed by two alpha helices, on which two longer helices form the inner surface of an open furrow, representing the binding site, and two small beta sheets serve as the outer walls of this furrow. Compound **1** is situated in the binding site, with its two chlorophenyl groups inserted into the hydrophobic interior of the site. Its isopropoxy group is also inserted into the hydrophobic cleft. The piperizine substituent appended to N1 of the imidazoline ring produced no intramolecular or intermolecular NOEs, so its position could not be determined. Since the lack of NOEs suggested that this moiety was fully flexible and located beyond contact with the protein, it is not depicted in the figures.

A more in-depth comparison of the hx-MDM2 protein to that from Xenopus shows that the intent of the design of the hybrid was essentially fulfilled. The backbone was not significantly altered by the three amino acid substitutions (RMSD for the backbone atoms including Cβ was 1.33 Å), so that the only consequential alteration was the replacement of the three key active site sidechains, as desired. The observation that the binding properties of the hybrid protein do not exactly match those of the human protein must be due to subtleties in the positions of these three sidechains, or to influences from remote sections of the protein where the amino acids have not been converted, although the nature of such influences are not obvious from the structure.

*Detailed examination of the binding strategy exhibited by compound **1***

The interactions that Compound **1** makes with MDM2 are predominantly hydrophobic. One of the chlorophenyl groups is deeply embedded into the core of the protein, surrounded by aromatic and methyl-containing residues – Leu50, Leu53, Ile57, Phe82, Phe87, Val89, Ile95, and Met98. The other chlorophenyl group is in a similar environment, although not embedded as deeply, surrounded by Leu50, Val89, His92, and Ile95. These moieties of the inhibitor achieve good shape complementarity with the side chains of the active site. It appears that the rigidity and geometry of the inhibitor contribute to effective binding, by forcing the two chlorophenyls down into the core of the protein and imposing a relative orientation that is well-positioned with respect to the two subpockets.

The imidazoline ring sits at the top of the binding site and appears to serve as a miniature lid between

the hydrophobic pockets below and the solvent above. As previously mentioned, the piperazine ring attached to N1 of the imidazoline must be projecting into the solvent, as it appears to be completely flexible and not in contact with the protein.

The third aromatic ring attached to the imidazoline is also situated along the top of the binding site. From this position, its isopropoxy substituent is able to access a third hydrophobic subpocket of the site. In this subpocket, the isopropoxy group is surrounded by aromatic and methyl-containing side chains – Ile57, Met58, Tyr63, and Val71. The shape complementarity achieved at this subsite is reasonably close-fitting. The methoxy substituent does not occupy a specifically-formed subsite, but does make contact with the Cα of Gln68 and the Cα and Cβ of His69.

*Comparison between compound **1** and a peptide ligand*

An overlay of the bound structure of Compound **1** with that of the bound p53 peptide, taken from the published X-ray structure (Kussie et al., 1996), is shown in Figure 5. It is clear from this superposition that the three peptide side chains shown to be most important for activity are successfully mimicked by Compound **1**. Leu26 and Trp23 are mimicked by the two chlorophenyl groups, and Phe19 is mimicked by the isopropoxy group. One can also envision that a 6-chloro substitution on Trp23, which was shown to impart increased binding affinity (Garcia-Echeverria et al., 2000), is, by analogy, already present on Compound **1**.

This is the first system involving a small molecule inhibitor of a protein-protein interaction in which high resolution complex structures are available for both the inhibitor and the natural ligand it is meant to emulate. A significant conclusion from this comparison is that, for a binding site like the present one, a successful peptidomimetic need not precisely duplicate the peptide backbone. In this case, the alpha helical backbone is simply serving as a rigid scaffold which presents the sidechains in a particular spatial orientation. A second significant finding is that the imidazoline core of Compound **1** is able to economically bridge an 8-residue segment of an alpha helix. That is, residues as far apart as Phe19 and Leu26 are effectively replaced by appendages from this core. The important overall learning is that there is nothing exceptional needed to inhibit a protein-protein interaction – the general rule is followed: if a molecule can properly mimic the key interactions made by a natural ligand, it can be an effective and potent inhibitor.

Implications of the structure for drug design

The NMR structure of the complex between hx-MDM2 and Compound **1** represents one landmark along our drug discovery endeavor to find an inhibitor of the MDM2-p53 interaction. A more complete description of this endeavor is beyond the scope of this discourse and will be the subject of separate reports. However, it is clear that two design issues are immediately addressed by the structure: why does Compound **1** show thirty-fold lower binding activity than the best peptide ligands, and what opportunities are revealed for improving the affinity of Compound **1**? The lower affinity of Compound **1** might be explainable by the observation that it does not accurately mimic Leu22, one of the minor contact residues of the p53 peptide, thereby not filling as many subpockets as does the peptide. Position 22 was found to be a location where affinity could be increased via substitution with tyrosine, and increased even further via replacement with phosphonomethylphenylalanine (Garcia-Echeverria et al., 2000). This suggests the presence of a reasonably sized subpocket in this region of the binding site, featuring some hydrophobic character and a positive charge available at one end for a charge-charge interaction. Therefore, one apparent strategy for increasing the affinity of Compound **1** would be to fully access this pocket with a group that would match the specific interaction opportunities available therein. The most direct way to accomplish this strategy would be to exploit a finding derived from the overlay of the two ligands – the methoxy substituent of Compound **1** already partially overlays the side chain of Leu22. Appending more elaborate groups to Compound **1** in place of the methoxy might lead to more total contact and better complementarity at this subpocket, resulting in tighter binding. The structure can serve as a guide for choosing substituents that would fit most appropriately.

Conclusion

A high-resolution NMR structure has been presented for a complex between a small molecule inhibitor and a specially engineered construct of MDM2 that represents a hybrid between the human and Xenopus forms. The inhibitor binds in the same site as does a

peptide ligand representing a fragment of the natural binding partner p53. The inhibitor is able to successfully mimic the peptide by duplicating interactions normally made by three sidechains within subpockets on the protein, and by utilizing a scaffold that presents substituents with rigidity and spatial orientation comparable to that provided by the alpha helical backbone of the peptide. The structure has been used to generate ideas for further increasing the binding potency of the inhibitor.

NMR resonance assignments have been deposited in the BioMagResBank (accession number 6248). Coordinates for the final ensemble of 18 structures have been deposited in the Protein Data Bank (PDB ID-code 1TTV).

Acknowledgements

We thank our colleagues Bradford Graves and Sung-Sau So for helpful input.

References

Arkin, M.R., Randal, M., DeLano, W.L., Hyde, J., Luong, T.N., Oslob, J.D., Raphael, D.R., Taylor, L., Wang, J., McDowell, R.S., Wells, J.A. and Braisted, A.C. (2003) *Proc. Natl. Acad. Sci. USA*, **100**, 1603–1608.

Asada, S., Choi, Y. and Uesugi, M. (2003) *J. Am. Chem. Soc.*, **125**, 4992–4993.

Bax, A., Clore, G.M. and Gronenborn, A.M. (1990) *J. Magn. Reson.*, **88**, 425–431.

Berg, T. (2003) *Agnew. Chem. Int. Ed.*, **42**, 2462–2481.

Berg, T., Cohen, S.B., Desharnais, J., Sonderegger, C., Maslyar, D.J., Goldberg, J., Boger, D.L. and Vogt, P.K. (2002) *Proc. Natl. Acad. Sci. USA*, **99**, 3830–3835.

Bohacek, R.S., Dalgarno, D.C., Hatada, M., Jacobsen, V.A., Lynch, B.A., Macek, K.J., Merry, T., Metcalf, C.A., Narula, S.S., Sawyer, T.K., Shakespeare, W.C., Violette, S.M. and Weigele, M. (2001) *J. Med. Chem.*, **44**, 660–663.

Braisted, A.C., Oslob, J.D., Delano, W.L., Hyde, J., McDowell, R.S., Waal, N., Yu, C., Arkin, M.R. and Raimundo, B.C. (2003) *J. Am. Chem. Soc.*, **125**, 3714–3715.

Brinkmann, U., Mattes, R.E., Buckel, P. (1989) *Gene* **85**,109–114.

Bueso-Ramos, C.E., Yun, Y., deLeon, E., McCowm, P., Stass, S. and Albitar, M. (1993) *Blood*, **82**, 2617–2623.

Carter, P.H., Scherle, P.A., Muckelbauer, J.A., Voss, M.E., Liu, R.-Q., Thompson, L.A., Tebben, A.J., Solomon, K.A., Lo, Y.C., Li, Z., Strzemienski, P., Yang, G., Falahatpisheh, N., Xu, M., Wu, Z., Farrow, N.A., Ramnarayan, K., Wang, J., Rideout, D., Yalamoori, V., Domaille, P., Underwood, D.J., Trzaskos, J.M., Freidman, S.M., Newton, R.C. and Decicco, C.P. (2001) *Proc. Natl. Acad. Sci. USA*, **98**, 11879–11884.

Chen, J., Marechal, V. and Levine, A.J. (1993) *Mol. Cell. Biol.*, **13**, 4107–4114.

Chen, L., Tilley, J.W., Trilles, R.V., Yun, W., Fry, D., Cook, C., Rowan, K., Schwinge, V. and Campbell, R. (2002) *Bioorg. Med. Chem. Lett.*, **12**, 137–141.

Clackson, T. and Wells, J.A. (1995) *Science*, **267**, 383–386.

Clore, G.M. and Gronenborn, A.M. (1994) In *Methods in Enzymology,* Vol. 239*: Nuclear Magnetic Resonance*, Part C, James, T.L. and Oppenheimer, N.J. (Eds.), Academic Press, San Diego, pp. 349–363.

Cornilescu, G., Delaglio, F. and Bax, A. (1999) *J. Biomol. NMR*, **13**, 289–302.

Emerson, S.D., Madison, V.S., Palermo, R.E., Waugh, D.S., Scheffler, J.E., Tsao, K.-L., Kiefer, S.E., Liu, S.P. and Fry, D.C. (1995) *Biochemistry*, **34**, 6911–6918.

Emerson, S.D., Palermo, R., Liu, C.-M., Tilley, J.W., Chen, L., Danho, W., Madison, V.S., Greeley, D.N., Ju, G. and Fry, D.C. (2003) *Protein Sci.*, **12**, 811–822.

Gadek, T.R., Burdick, D.J., McDowell, R.S., Stanley, M.S., Marsters, J.C., Paris, K.J., Oare, D.A., Reynolds, M.E., Ladner, C., Zioncheck, K.A., Lee, W.P., Gribling, P., Dennis, M.S., Skelton, N.J., Tumas, D.B., Clark, K.R., Keating, S.M., Beresini, M.H., Tilley, J.W., Presta, L.G. and Bodary, S.C. (2002) *Science*, **295**, 1086–1089.

Garcia-Echeverria, C., Chene, P., Blommers, M.J.J. and Furet, P. (2000) *J. Med. Chem.*, **43**, 3205–3208.

Haupt, Y., Maya, R., Kazaz, A. and Oren, M. (1997) *Nature*, **387**, 296–299.

Higuchi, R., Krummel, B. and Saiki, R.K. (1988) *Nucl. Acids Res.*, **16**, 7351–7367.

Ho, S.N., Hunt, H.D., Horton, R.M., Pullen, J.K. and Pease, L.R. (1989) *Gene*, **77**, 51–59.

Hollstein, M., Sidransky, D., Vogelstein, B. and Harris, C.C. (1991) *Science*, **253**, 49–53.

Ikura, M. and Bax, A. (1992) *J. Am. Chem. Soc.*, **114**, 2433–2440.

Jennerwein, M., Wappes, B., Gust, R., Schonenberger, H., Engel, J., Seeber, S. and Osieka, R. (1988) *J. Can. Res. Clin. Oncol.*, **114**, 347–358.

Johnson, B.A. and Blevins, R.A. (1994) *J. Biomol. NMR*, **4**, 603–614.

Kallen, J., Weizenbach, K., Ramage, P., Geyl, D., Kriwacki, R., Legge, G., Cottens, S., Weitz-Schmidt, G. and Hommel, U. (1999) *J. Mol. Biol.*, **292**, 1–9.

Kay, L.E., Keifer, P. and Saarinen, T. (1992) *J. Am. Chem. Soc.*, **114**, 10663–10665.

Ku, T.W., Ali, F.E., Barton, L.S., Bean, J.W., Bondinell, W.E., Burgess, J.L., Callahan, J.F., Calvo, R.R., Chen, L., Eggleston, D.S., Gleason, J.G., Huffman, W.F., Hwang, S.M., Jakas, D.R., Karash, C.B., Keenan, R.M., Kopple, K.D., Miller, W.H., Newlander, K.A., Nichols, A., Parker, M.F., Peishoff, C.E., Samanen, J.M., Uzinskas, I. and Venslavsky, J.W. (1993) *J. Am. Chem. Soc.*, **115**, 8861–8862.

Kubbutat, M.H.G., Jones, S.N. and Vousden, K.H. (1997) *Nature*, **387**, 299–303.

Kussie, P.H., Gorina, S., Marechal, V., Elenbaas, B., Moreau, J., Levine, A.J. and Pavletich, N.P. (1996) *Science*, **274**, 948–953.

Laskowski, R.A., Rullmann, J.A.C., MacArthur, M.W., Kaptein, R. and Thornton, J.M. (1996) *J. Biomol. NMR*, **8**, 477–496.

Last-Barney, K., Davidson, W., Cardozo, M., Frye, L.L., Grygon, C.A., Hopkins, J.L., Jeanfavre, D.D., Pav, S., Qian, C., Stevenson, J.M., Tong, L., Zindell, R. and Kelly, T.A. (2001) *J. Am. Chem. Soc.*, **123**, 5643–5650.

Levine, A.J. (1997) *Cell*, **88**, 323–331.

Liu, G., Huth, J.R., Olejniczak, E.T., Mendoza, R., DeVries, P., Leitza, S., Reilly, E.B., Okasinski, G.F., Fesik, S.W. and von Geldern, T.W. (2001) *J. Med. Chem.*, **44**, 1202–1210.

Lunney, E.A., Para, K.S., Rubin, J.R., Humblet, C., Fergus, J.H., Marks, J.S. and Sawyer, T.K. (1997) *J. Am. Chem. Soc.*, **119**, 12471–12476.

Marchetti, A. (1995) *J. Pathol.*, **173**, 31–38.
McCoy, M.A. and Mueller, L. (1992) *J. Am. Chem. Soc.*, **114**, 2108–2112.
McDowell, R.S., Blackburn, B.K., Gadek, T.R., McGee, L.R., Rawson, T., Reynolds, M.E., Robarge, K.D., Somers, T.C., Thorsett, E.D., Tischler, M., Webb, R.R. and Venuti, M.C. (1994) *J. Am. Chem. Soc.*, **116**, 5077–5083.
McMillan, K., Adler, M., Auld, D.S., Baldwin, J.J., Blasko, E., Browne, L.J., Chelsky, D., Davey, D., Dolle, R.E., Eagen, K.A., Erickson, S., Feldman, R.I., Glaser, C.B., Mallari, C., Morrissey, M.M., Ohlmeyer, M.H.J., Pan, G., Parkinson, J.F., Phillips, G.B., Polokoff, M.A., Sigal, N.H., Vergona, R., Whitlow, M., Young, T.A. and Devlin, J.J. (2000) *Proc. Natl. Acad. Sci. USA*, **97**, 1506–1511.
Midgley, C.A. and Lane, D.P. (1997) *Oncogene*, **15**, 1179–1189.
Muhandiram, D.R. and Kay, L.E. (1994) *J. Magn. Reson.*, **103**, 203–216.
Nagayama, K. (1986) *J. Magn. Reson.*, **66**, 240–249.
Nilges, M. Clore, G.M. and Gronenborn, A.M. (1988a) *FEBS Lett.*, **239**, 129–136.
Nilges, M., Gronenborn, A.M., Brunger, A.T. and Clore, G.M. (1988b) *Protein Eng.*, **2**, 27–38.
Oliner, J.D., Kinzler, K.W., Meltzer, P.S., George, D. and Vogelstein, B. (1992) *Nature*, **358**, 80–83.
Orner, B.P., Ernst, J.T. and Hamilton, A.D. (2001) *J. Am. Chem. Soc.*, **123**, 5382–5383.
Picksley, S.M., Vojtesek, B., Sparks, A. and Lane, D.P. (1994) *Oncogene*, **9**, 2523–2529.
Proudfoot, J. R., Betageri, R., Cardozo, M., Gilmore, T.A., Glynn, S., Hickey, E.R., Jakes, S., Kabcenell, A., Kirrane, T.M., Tibolla, A.K., Lukas, S., Patel, U.R., Sharma, R., Yazdanian, M. and Moss, N. (2001) *J. Med. Chem.*, **44**, 2421–2431.
Reifenberger, G., Lu, L., Ichimura, K., Schmidt, E.E. and Collins, V.P. (1993) *Cancer Res.*, **53**, 2736–2739.
Rutledge, S.E., Chin, J.W. and Schepartz, A. (2002) *Curr. Opin. Chem. Biol.*, **6**, 479–485.
Shaka, A.J., Lee, C.J. and Pines, A. (1988) *J. Magn. Reson.*, **77**, 274–293.
Shibagaki, I., Tanaka, H., Shimada, Y., Wagata, T., Ikenaga, M., Imamura, M. and Ishizaki, K. (1995) *Clin. Cancer Res.*, **1**, 769–773.
Smith, A.B., Hirshmann, R., Pasternak, A., Yao, W., Sprengeler, P.A., Holloway, M.K., Kuo, L.C., Chen, Z., Darke, P.L. and Schleif, W.A. (1997) *J. Med. Chem.*, **40**, 2440–2444.
Stoll, R., Renner, C., Hansen, S., Palme, S., Kelin, C., Belling, A., Zeslawski, W., Kamionka, M., Rehm, T., Muhlhahn, P., Schumacher, R., Hesse, F., Kaluza, B., Voelter, W., Engh, R. and Holak, T. (2001) *Biochemistry*, **40**, 336–344.
Stonehouse, J., Shaw, G.L., Keeler, J. and Laue, E.D. (1994) *J. Magn. Reson.*, **107**, 178–184.
Tilley, J.W., Chen, L., Fry, D.C., Emerson, S.D., Powers, G.D., Biondi, D., Varnell, T., Trilles, R., Guthrie, R., Mennona, F., Kaplan, G., LeMahieu, R.A., Carson, M., Han, R.-J., Liu, C.-M., Palermo, R. and Ju, G. (1997) *J. Am. Chem. Soc.*, **119**, 7589–7590.
Toogood, P.L. (2002) *J. Med. Chem.*, **45**, 1543–1558.
Vogtle, F. and Goldschmitt, E. (1976) *Chem. Ber.*, **109**, 1–40.
Zheleva, D.I., Lane, D.P. and Fischer, P.M. (2003) *Mini Rev. Med. Chem.*, **3**, 257–270.
Zhu, Y.-F., Wang, X.-C., Connors, P., Wilcoxen, K., Gao, Y., Gross, R., Strack, N., Gross, T., McCarthy, J.R., Xie, Q., Ling, N. and Chen, C. (2003) *Bioorg. Med. Chem. Lett.*, **13**, 1931–1934.